

Texture Analysis of Directionally-Solidified Si Films Obtained via Line-Scan SLS

A.M. Chitu*, P.C. van der Wilt, U.J. Chung, B.A. Turk, V.M. McCreary, A.B. Limanov, and James S. Im

Program in Materials Science and Engineering, Department of Applied Physics and Applied Mathematics, Columbia University, New York, NY, USA

Phone: +1-212-8547861, E-mail: ac2224@columbia.edu

Abstract

Directionally solidified Si films obtained via line-scan SLS can lead to attainment of high-mobility TFTs. The crystallographic texture of the resultant materials can potentially be an important factor because the spatial details thereof may impact the overall device uniformity. Here, we present EBSD analysis of these materials that reveal the existence of relatively large domains with different textures and differing amounts of defects, which in turn, may adversely affect device uniformity.

1. Introduction

Sequential lateral solidification (SLS) is a pulsed-laser-based crystallization method that was introduced over a decade ago [1]. The method has evolved and progressed to the point where, in recent years, a particular scheme of the method that utilizes multiple beamlets to produce a uniform large-grain polycrystalline microstructure (referred as “2-shot” SLS material) has been successfully implemented in mass production of low-temperature polycrystalline Si (LTPS) AMLCDs [2]. Overall, SLS has demonstrated itself to be an exceptionally flexible approach, which can be configured to produce various low-defect-density/large-grain polycrystalline Si (poly-Si) materials as well as location-controlled single-crystal regions using a number of different system configurations and experimental procedures.

Technically, SLS can be described as an iterative process that involves two fundamental steps: (1) pulsed-laser irradiation to induce localized complete melting of the Si film followed by lateral solidification from unmelted seeds situated at the periphery of the melt, and (2) precise beam or sample translation followed by re-irradiation to induce epitaxial lateral growth to proceed from previously laterally grown grains.

One particularly straightforward way to implement SLS involves using a single line beam that is scanned over the film typically at a constant scan-velocity/laser-frequency combination. This particular SLS scheme in which a single beam is utilized, was first presented and demonstrated in 1998, and is

generally referred to as line-scan SLS [3]. This process is noteworthy because it can be utilized (1) to at least create a material with directionally solidified microstructure (by keeping the sample translation distance between the pulses to be less than the single-shot induced lateral growth distance) over the entire beam-scanned area, as well as (2) to also create the aforementioned 2-shot SLS microstructure (by preventing any nucleation to take place within the irradiated area and by keeping the sample translation distance between the pulses to be greater than the single-shot-induced lateral-growth distance and less than twice that value) [4].

When optimally matched with high-repetition-rate/high-power pulsed lasers, the line-scan SLS approach holds definite promise in low-cost high-throughput production of advanced active-matrix LCDs and OLED displays [5].

Over the years, it has been demonstrated by several groups that high-performance LTPS thin-film transistors (TFTs) can be obtained from SLS-processed materials with directionally solidified microstructure when the source-to-drain direction (i.e., the current flow) is aligned approximately parallel to the elongated direction of the grains [6, 7, 4, 8]. However, it was also found that the uniformity of these high-mobility TFTs could be, at least for certain processing conditions and sample configurations, actually not as good as those obtained from the 2-shot material *obtained also via the line-scan SLS process* [4]. The physical reason behind this observation has not yet been established. One potential microstructure-related cause corresponds to the spatial variation in the surface crystal orientation of the grains and subgrains that make up the directionally solidified material.

In this paper, we present preliminary experimental findings regarding the spatially resolved crystallographic orientation of directionally solidified Si films obtained via line-scan SLS as determined through electron backscatter diffraction (EBSD). In particular, we present and elaborate on the occurrence of large domains consisting of crystallographically related grains and subgrains having similar in-plane

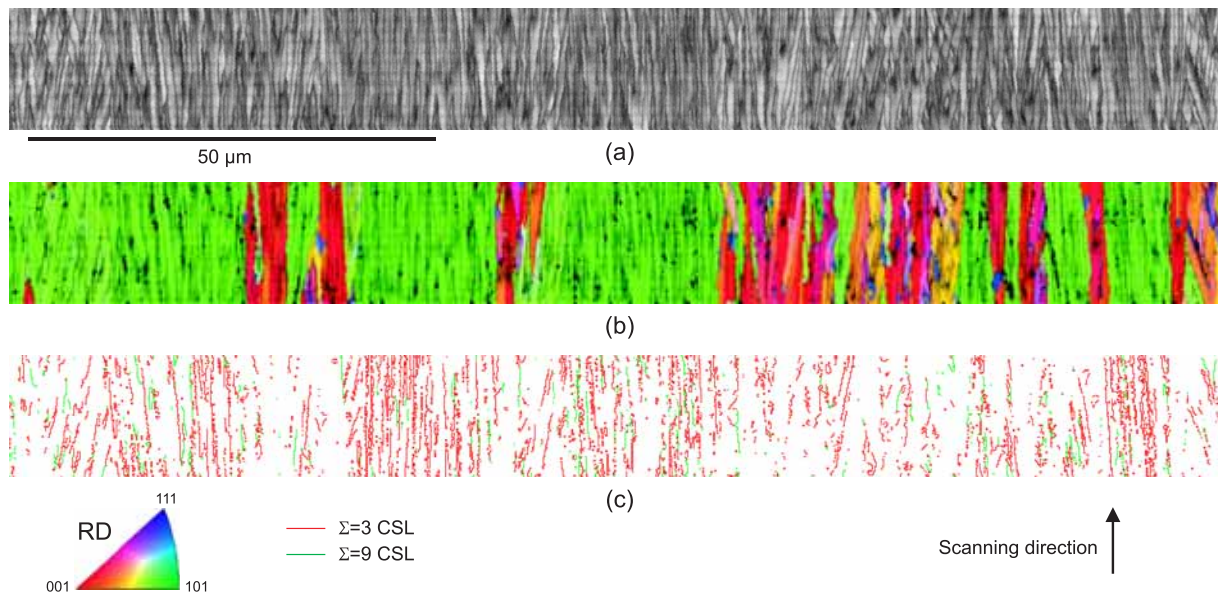


Figure 1: Three representations of a $150 \times 15 \mu\text{m}^2$ EBSD scan of a directionally solidified 100 nm Si film with a $1.2 \mu\text{m}$ step distance: (a) the “band-contrast” to visualize the microstructure; (b) the rolling-direction orientation with the band-contrast image superimposed and black regions indicating unresolved data points (after extrapolation); and (c) a map showing the distribution of several geometrically special grain boundaries.

orientations. (Although the presence of such domains has been experimentally noted previously [9], they have not been systematically analyzed nor related to the overall texture [10, 11] of the material.)

2. Experimental

The samples that were utilized in this study consisted of 100 nm thick amorphous Si (a-Si) films deposited on SiO_2 -coated glass substrates. SLS was performed using a projection-irradiation system capable of imaging chromium-on-quartz mask patterns with high resolution. The setup consisted of an excimer laser operating at 308 nm (XeCl), a pulse duration extender for elongating the pulse to $\sim 220\text{ns}$ (FWHM), a $5\times$ demagnification imaging system, and a submicron-precision translation stage. The beam was patterned into a ~ 1 mm long and 3.5, 5.0, or $6.5 \mu\text{m}$ wide line beam.

The samples were irradiated at $\sim 1.01 \text{ J/cm}^2$, which corresponds to about 1.5 times the energy density required to reach complete melting of the film. The irradiated regions were fully laterally crystallized (i.e., no nucleation occurred within the irradiated region) and lateral growth length was measured to be ~ 1.5 , ~ 2.2 , and $\sim 3.0 \mu\text{m}$ for the 3.5, 5.0, and $6.5 \mu\text{m}$ wide beams, respectively. The samples were irradiated at a fixed laser repetition rate of 50 Hz and with stage velocity adjusted to obtain in-between-pulse

translation distances (henceforth referred to as “step distance”) of 0.4 and $0.8 \mu\text{m}$ using the $3.5 \mu\text{m}$ wide beam; 1.2 and $1.6 \mu\text{m}$ using the $5.0 \mu\text{m}$ wide beam; and $2.0 \mu\text{m}$ using the $6.5 \mu\text{m}$ wide beam.

Crystallographic orientation characterization was performed using a JEOL JSM-5600 scanning-electron microscope (SEM) equipped with an electron backscatter diffraction (EBSD) system from HKL. The analytical software provided by the same source was used to “clean up” the data by removing singular data points followed by minor interpolation to remove missing data points.

3. Results

EBSD results that reveal the spatial distribution of the in-plane orientations in the direction of the scan (referred to hereafter as the rolling direction, RD) are shown in Figure 1. This particular set of data was taken from a region in the SLS-processed film (using a $1.2 \mu\text{m}$ step distance) that was located more than 8 mm from the start of the scan. It can be deduced from Figure 1(c) that two types of domains can be distinguished: those that have (110) RD texture and those that have (100) RD texture. The widths of these domains (which typically consist at least of multiple subgrains) can reach 10s of μm . Close examination of Figure 1(c) further reveals that $\langle 110 \rangle$ RD-oriented domains contain an apparently high density of $\Sigma=3$

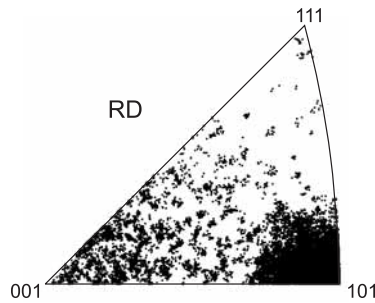


Figure 2: IPF of the RD orientation distribution in a directionally solidified 100 nm Si film with a 1.2 μm step distance obtained via EBSD over the entire width of the crystallized region.

coincident-site lattice (CSL) boundaries (i.e., first-order twin boundaries) that are aligned essentially parallel to the direction of growth.

The inverse-pole figure (IPF) data shown in Figure 2 were obtained from the same sample after the same scan distance but acquired over the entire 1 mm width of the crystallized region. The data reveal that the orientation distribution around the $\langle 110 \rangle$ pole is relatively tight, while the orientation distribution around the $\langle 100 \rangle$ pole is apparently more diffuse.

The mostly bimodal nature of the RD orientation distribution was observed for all experimental conditions investigated in the present study. The area fractions of the (100) RD textured and (110) RD textured regions, however, were found to depend on the step distance employed in the SLS scan. This dependence is revealed in Figure 3 where the fractions of data points within 15° of the $\langle 100 \rangle$ and $\langle 110 \rangle$ poles are shown in red and green, respectively. To better accommodate the more diffuse orientation distribution around the $\langle 100 \rangle$ pole, data points within 15° to 30° of $\langle 100 \rangle$ are shown in yellow. It can be seen that the fraction of (100) RD texture becomes significant for small step distances, while the fraction of (110) RD texture becomes dominant for longer step distances.

Although the tendency to form strong texture is observed primarily in the rolling direction, an examination of the orientation distribution in the other orthogonal directions reveals that some degree of texture formation also exists in these directions. The orientation distribution in all three directions (surface normal direction (ND), RD, and the in-plane direction perpendicular to the scanning direction referred to as transverse direction, TD) obtained over the entire width of the scanned area are shown in Figures 4 (a) and (b) for a step distance of 0.8 μm and 2.0 μm , respectively, as examples of a predominantly (100)

RD-textured film and a predominantly (110) RD-textured film (with other orientations shown in gray). In the former, the surface orientation shows a weak preference for $\{110\}$, while in the latter there is a preference for $\langle 111 \rangle$ in the transverse direction, which corresponds to a surface orientation of $\{112\}$.

4. Discussion

One important — and increasingly critical — aspect of LTPS TFTs is the overall uniformity of the device characteristics. In general, device non-uniformity can result from variations in the types and concentrations of structural defects as well as the crystallographic orientation(s) of grain(s) found within the active channel regions of devices. The surface-crystal-orientation dependent factors such as the Si-SiO₂ interface-state density [12] and the field-effect carrier mobility [13] have been demonstrated to affect the performance characteristics of devices.

For relatively “small-grain” materials (i.e., poly-Si films with grains substantially smaller than the active channel dimensions) the non-uniformity problem caused by grain-orientation-dependent effects may be largely circumvented even for randomly oriented grains, as there should be statistical sampling and averaging of variously orientated grains within one channel region. (Here, the contributions from individual grains will be statistically averaged over the large number of crystallographically unrelated grains that reside within the active channel area.)

For “large-grain” polycrystalline materials, however, such averaging effect may not sufficiently take place to prevent the contributions from individual grains to have a noticeable influence on the resulting device performance characteristics. (Such a situation appears to have been encountered for large-grain

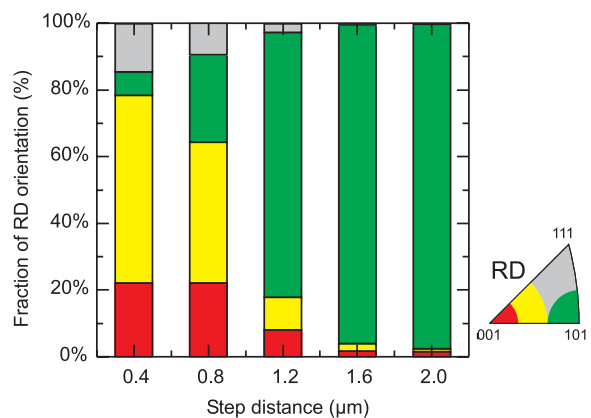


Figure 3: histogram showing the relative fraction of (100) and (110) RD-textured material as a function of step distance.

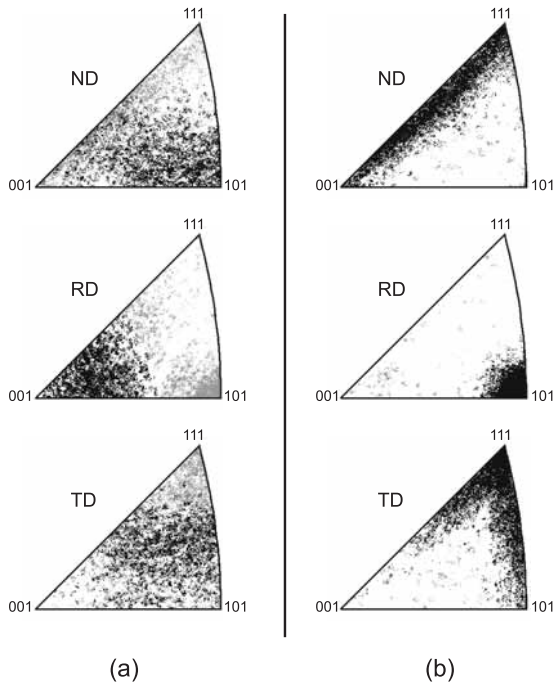


Figure 4: IPFs obtained via EBSD of (a) 0.8 μm step distance and (b) 2.0 μm step distance.

materials obtained via single-pulse-induced lateral growth where large TFT performance variation was observed as a function of surface orientation and intra-grain defect density [14].) The results presented in this paper suggest that a somewhat similar situation may potentially arise for the TFTs that are fabricated on directionally solidified materials obtained via line-scan SLS, as the directionally solidified materials were observed to typically consist of a mixture of two types of domains that differ in texture ((110) RD texture or (100) RD texture) and that have dimensions comparable to those of the active-channel area.

Furthermore, and likely more significantly, it has been observed that there exist distinct differences in the type, density, and distribution of planar defects that are found between these two types of domains (a more detailed discussion of this subject is presented elsewhere in these proceedings [15]). Taking these differences in account, one can conclude that, since it is exceedingly unlikely that these domains result in effectively identical device characteristics, the overall uniformity of TFTs that are fabricated on the directionally solidified materials can only be adversely affected by the coexistence of both (110) RD-textured and (100) RD-textured domains in the material.

Still, we are hopeful that a further analysis and understanding as regards the details of texture

development and defect formation during the line-scan SLS process should enable one to subsequently optimize and modify the process so as to yield improved materials. Alternatively, these texture- and defect-related results for directional line-scan SLS also point to the 2-shot line-scan SLS approach [4] as a technically attainable solution that has already been demonstrated to provide more uniform TFTs; the approach can be recognized, furthermore, to substantially improve other process-related factors (e.g. energy-density process window, effective crystallization rate/throughput, manufacturing cost, etc.) that are considered as being important as far as manufacturing is concerned.

5. Conclusions

The orientation-related experimental findings presented in this paper suggest that, at least for the parameter space that was examined in this work, the directionally solidified material obtained via line-scan SLS appears to possess crystallographic texture characteristics that could potentially affect the overall device uniformity in an unfavorable manner. Specifically, the analysis reveals the coexistence of relatively large crystallographically textured domains — which are furthermore populated with different types of planar defects — with characteristic dimensions at least on the order of (or often much wider than) the typical active-channel regions.

6. Acknowledgements

This work was in part supported by DARPA-funded, AFRL-managed Microelectronics Program Contract FA8650-04-C-7101, by Samsung Electronics, Inc., and by Cymer, Inc.

7. References

- [1] R.S. Sposili and J.S. Im, *Appl. Phys. Lett.* **69**, 2864 (1996).
- [2] C.W. Kim, K.C. Moon, H.J. Kim, K.C. Park, C.H. Kim, I.G. Kim, C.M. Kim, S.Y. Joo, J.K. Kang, and U.J. Chung, *Proc. SID* **35**, 868 (2004).
- [3] R.S. Sposili and J.S. Im, *Appl. Phys. A* **67**, 273 (1998).
- [4] S.D. Brotherton, M.A. Crowder, A.B. Limanov, B.A. Turk, and J.S. Im, *Proc. IDRC* **21**, 387 (2001).
- [5] D.S. Knowles, J.Y. Park, C. Im, P. Das, T. Hoffman, B. Burfeindt, H. Muenz, A. Herkommer, P.C. van der Wilt, A.B. Limanov, and J.S. Im, *Proc. SID* **36**, 503 (2005).
- [6] Y.H. Jung, J.M. Yoon, M.S. Yan, W.K. Park, H.S. Soh, H.S. Cho, A.B. Limanov, and J.S. Im, *Proc. MRS* **621**, Q8.3.1 (2000).

- [7] R. Dassow, J. Koehler, M. Nerding, H.P. Strunk, Y. Helen, K. Mourgues, O. Bonnaud, T. Mohammed-Brahim, and J.H. Werner, *Proc. MRS* **621**, Q9.3.1 (2000).
- [8] A.T. Voutsas, *IEEE Trans. Electron Devices* **50**, 1494 (2003).
- [9] A.B. Limanov, V.A. Chubarenko, V.M. Borisov, A.Y. Vinokhodov, A.I. Demin, O.B. Khristoforov, A.V. El'tsov, and Y.B. Kiryukhin, *Russ. Microelectron.* **28**, 25 (1999).
- [10] M. Nerding, S. Christiansen, J. Krinke, R. Dassow, J.R. Köhler, J.H. Werner, and H.P. Strunk, *Thin Solid Films* **383**, 110 (2001).
- [11] A.T. Voutsas, A.B. Limanov, and J.S. Im, *J. Appl. Phys.* **94**, 7445 (2003).
- [12] J.R. Ligenza, *J. Phys. Chem.*, **65**, 2011 (1961).
- [13] T. Sato, Y. Takeishi, H. Hara, and Y. Okamoto, *Phys. Rev. B* **4**, 1950 (1971).
- [14] A.T. Voutsas, presented at *E-MRS*, Nice, France, (June 2006).
- [15] U.J. Chung, A.B. Limanov, M.A. Crowder, P.C. van der Wilt, A.M. Chitu, and J.S. Im, these proceedings.